CYBERNETICS AND PHYSICS, VOL. 3, NO. 2, 2014 , 73–78

COMPUTER SIMULATION OF RESIDUAL GAS IONIZATION IN GAS-FILLED NEUTRON TUBES

Vladimir I. Rashchikov
Department of Electrophysical Facilities
National Research Nuclear University (MEPHI)
Russia
VIRashchikov@mephi.ru

Abstract

Deuteron beam acceleration in ion-optic system of gas-filled neutron tubes was investigated. Particle in cell (PIC) code SUMA [Rashchikov, 1990] [Didenko, Rashchikov and Fortov, 2011] used for computer simulation of ionization and knock on processes and there influence on deuteron beam parameters. When deuteron and ionized particles space charge self-field forces become the same order of magnitude as external one, virtual cathode may occurs. It is happens because of injected from ion source deuterons cannot overcome their own space charge potential wall and move in transverse direction. However, electrons, produced by ionization, are trapped within the deuteron beam space charge potential wall and decrease it significantly. Thus, space charge neutralization of deuteron beams by electrons, may considerably increase target current and, as a result, output neutron flow. Moreover, own longitudinal electric field rise near the target leads to reduction of accelerating electrode target potential wall, which was made to prevent knock on emission from the target. As a result, additional knocked on electrons may appear in the region and should be taken into account. The data obtained were compared with experimental results.

Key words

Computer simulation, ion-optic system, ionization, neutron tubes.

1 Introduction

To design neutron tube with assigned flow value and other parameters such as size, service life and so forth, preliminary computer simulation should be fulfilled. PIC code SUMA was used for ion-optic system modeling and investigation of ionization processes influence on deuteron beam dynamics and output data of gas-filled neutron tubes.

The main purpose of this paper is investigation of ionization processes influence on deuteron beam dynamics and output data of gas-filled neutron tubes.

2 Code SUMA

For numerical simulation relativistic PIC code solving complete system of Maxwell equation is used. The code is a 2.5 dimensional time dependent model that makes it possible to describe self-consistently the dynamics of charged particles in rectangular, cylindrical, and polar systems of coordinates.

The system of equations used in mathematical model consists of the Maxwell equations, the equation of the medium, and the equation of motion. At each step of the solution at running instant t, the charge and current densities appearing in the Maxwell equations are calculated first. The charges and current are distributed among the nodes of the spatial mesh and smoothed by weighing the areas of a particle (cloud) and a mesh. The arrival of new particles at a simulation step Δt to the region under investigation is simulated by the mechanism of injection, emission or secondary emission with corresponding laws of distribution. Then the Maxwell equations are solved numerically, and the resultant solution is corrected for matching to the Poisson equation. The correction is carried out by solving the Poisson equation for the difference of charge density distribution obtained from the divergence Maxwell equations and the actual distribution of charges ρ,

$$\Delta\Phi_c = \frac{-(\rho-\rho^*)}{\varepsilon} \tag{1}$$

where

$$div\,\vec{E} = \frac{\rho^*}{\varepsilon} \tag{2}$$

The corrected expression for the field has the form

$$\vec{E}_c = \vec{E} - grad(\Phi_c) \tag{3}$$

The Poisson equation is solved using the algorithm of fast Fourier transformation in one coordinate and marching (Thomas algorithm) in the other coordinate. For domains with a complex geometry as well as in the presence of electrodes in the domain, the capacity matrix method is used, which relates the potential and charge at the required nodes.

The following boundary conditions can be specified at the domain boundary:

(i) the conditions on the metal surface;

(ii) periodicity conditions;

(iii) symmetry conditions;

(iv) conditions for wave transmission.

Since the solutions of the Maxwell equations give the field at the nodes of 2D mesh, the field at the intermediate points at which particles are located must be calculated for numerical integration of the equations of motion. For this purpose, interpolation and smoothing of mesh functions is used. Integrating the equations of motion, we determine the distribution of particles in the phase space at the next instant $t + \Delta t$, and so on. For integration, the relativistic version of the method is employed with overstep using a time shift of the spatial coordinate and momentum. In the model, the energy balance in the domain under investigation is controlled:

$$P_{\sum} + \frac{\partial W}{\partial t} + P = 0 \qquad (4)$$

For this purpose, we evaluate on the mesh the integrals of the following form:

$$W = \frac{1}{2}\int(\vec{H}\vec{B} + \vec{E}\vec{D})dV \qquad (5)$$

which gives the value of energy stored in the domain; integral

$$P = \int\limits_{V} \vec{j}\vec{E}dV \qquad (6)$$

which makes it possible to estimate the power transformation in the system, and integral

$$P_{\sum} = \oint [\vec{E}\vec{H}]dS \qquad (7)$$

for evaluating the flux through the preset surface.

3 Computer Simulation

As a sample typical gas-filled pulse neutron tube has been studied (see Fig. 1).

Accelerated electrode is under -85 kV potential, target -83 kV, focusing electrode is grounded. Preliminary ion source deuteron beam parameters has been obtained experimentally. For this purpose alone Langmuir probes, multi-electrode energy analyzer and Faraday cup were used. We obtain following deuteron beam

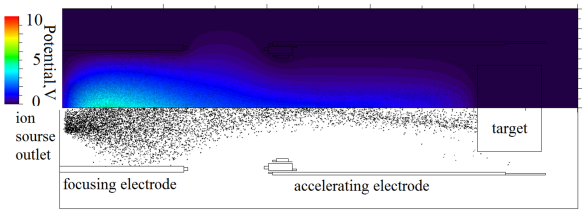

Figure 1: Deuterons distribution (lower) and their self-field potential (upper) in neutron tube.

parameter: longitudinal energy 1.7 $\pm$ 0.4 keV, current 150 μA for initial gas pressure 0.5×10^{-3} Torr. Moreover, some beam density distribution measurement were fulfilled. Nevertheless, it was not enough data for computer simulation. Therefore, the attempt to solve inverse problem was made. As the result to be obtained the experimental deuteron current density distribution on target shown on Fig. 2*a* was used. Experimental data were rebuild from target depth ero-

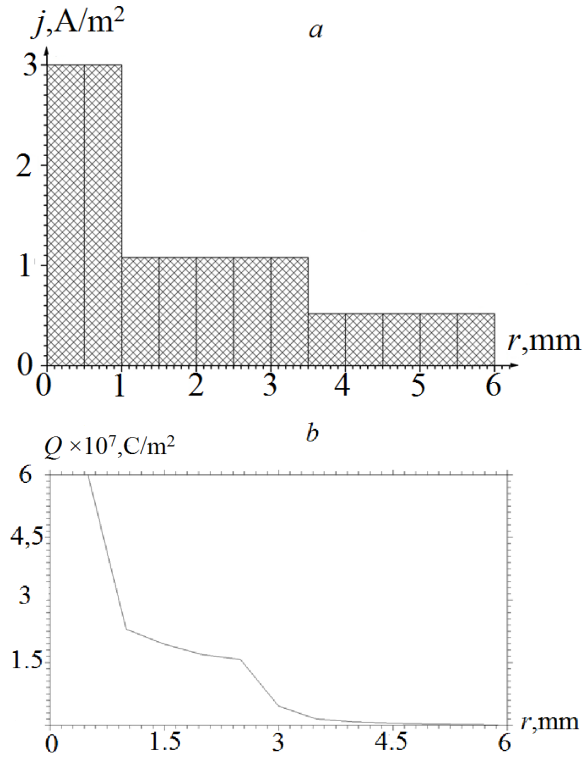

Figure 2: Current density (experimental, *a*) and charge distributions (simulation, *b*) on the target.

sion and target sputtering calculation. Computer simulation shows that for the following input beam data, experimental and calculated distributions are closed to each other: longitudinal energy 1.9 $\pm$ 0.1 keV and transverse energy distribution 120 eV, current 150 μA (see Fig. 2*b*). Fig. 3 shows deuteron beam filling out

neutron tube. Emittan measurement carried out a bit later shown on Fig. 4. 90% beam particles have angle divergence in the range $0.15 \div -0.10$, that corresponds to transverse energy distribution $\sim$120 eV, that is in a good agreement with computer simulation results.

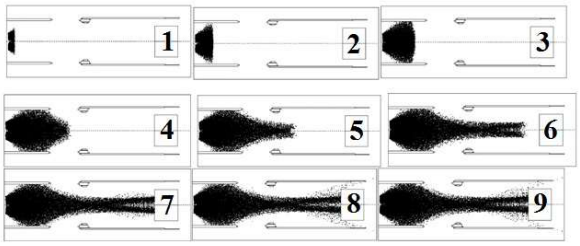

Figure 3: Deuteron beam filling out neutron tube. Time: 1 – 5 ns; 2 – 15 ns; 3 – 25 ns; 4 – 35 ns; 5 – 40 ns; 6 – 45 ns; 7 – 50 ns; 8 – 55 ns; 9 – 60 ns.

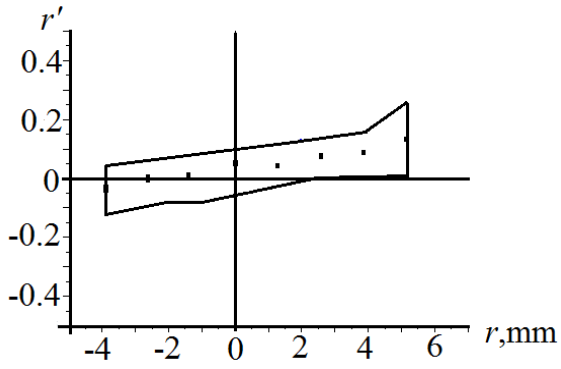

Figure 4: Beam emittane diagram

Once more possibility to compare computer simulation results with experimental data is using of luminous ion beam technique [Belikh et al., 1992], which based on visualization of excited ion beam trajectories. Fig. 5 shows ion beam photo in accelerating gap (*a*, *c*) and calculated space charge distribution (*b*, *d*) for the same beam current and accelerating voltage values. Bright part of this photos (*a*, *c*) is deuteron trajectories between focusing (left) and accelerating (right) electrodes. Pictures *a* and *b* correspond to accelerating electrode potential 60 kV, *c* and *d* – 0 kV.

Changing accelerating voltage and beam parameters, we compare the results, which are in a good agreement.

Computer simulation results comparison with experimental data let us obtain ion source output beam parameters with accuracy enough for the further ion optic system simulation.

Main purpose of this modeling was to choose potential distribution and electrodes geometry for uniform

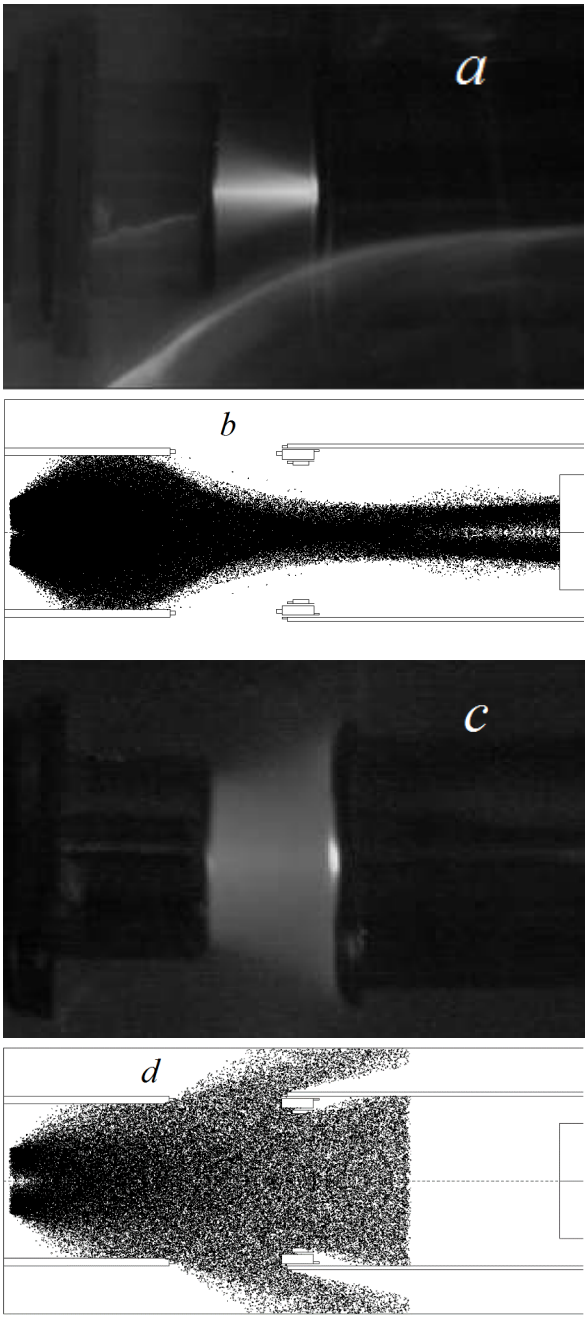

Figure 5: Beam photo (*a*, *c*) and calculated space charge distribution (*b*, *d*) in accelerating gap. Pictures *a* and *b* correspond to accelerating electrode potential 60 kV, *c* and *d* – 0 kV.

deuteron beam distribution on the target. This leads to target service life rise and, as a result, neutron tube durability has increased ether.

Fig. 6 shows target charge density distribution changing during target moves to right border. Potentials on the accelerating electrode and target are 85 kV and 83 kV respectively. Input deuteron beam parameters are the following: longitudinal energy 1.9 ± 0.1 keV, transverse energy distribution 120 eV, current 150 μA.

Compare Fig. 2*b* and Fig. 6 we make conclusion, that

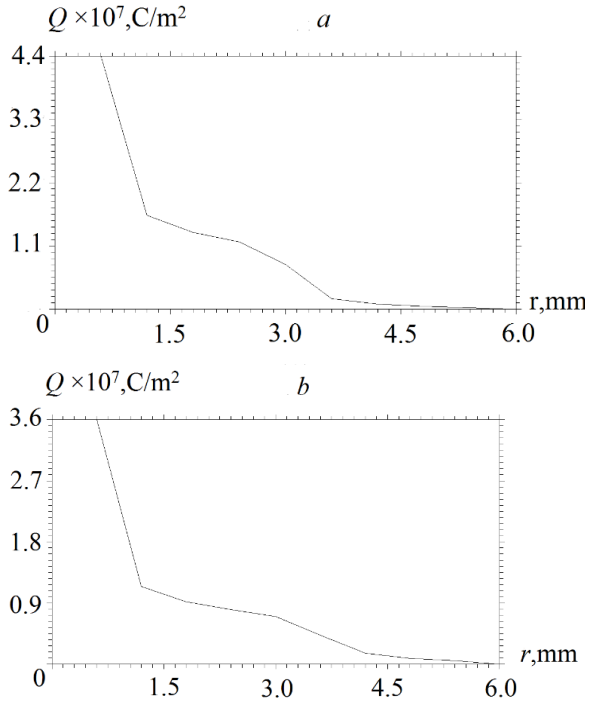

Figure 6: Target charge density distribution. Accelerating electrode potential 85 kV. *a* - target right shift 4.5 mm, *b* - target right shift 11.5 mm

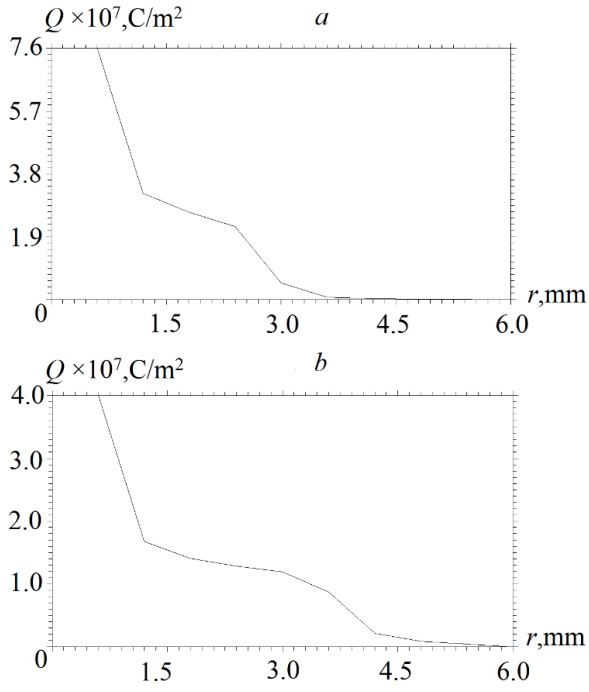

Figure 7: Target charge density distribution. Accelerating electrode potential 155 kV. *a* without target right shift, *b* - target right shift 11.5 mm

this is a way to improve uniformity of target charge density distribution.

One of the way to increase output neutron flow is accelerating voltage rise. But in this case to obtain uniform target charge distribution we need output ion source energy equal to 4 keV and accelerating electrode potential 155 kV (Fig. 7). Using this accelerating voltage, we may twice increase output neutron flow and have acceptable target charge density distribution.

4 Residual Gas Influence

Passing through the gas, deuteron beam produce plasma, which consist of electron and slow ion. Their densities under considered gas pressure range approximately equal each other (see Fig. 8) [Holmes, 1979] . Deuteron and ionized particles own space charge forces for this current value are considerably less than that of the external one (see Fig. 9.). The value of decelerating deuteron space charge self-field is about 1 kV/m, that three order of magnitude less than external accelerating field. Therefore, they cannot effect on deuteron beam propagation. Figure 10 shows that electric field is accelerating for the deuteron elsewhere in the tube. The electrons knocked on from the target by accelerated deuterons cannot pass through the accelerating electrode target potential wall and cannot effect on deuteron beam propagation either (see Fig. 11).

Current gain leads to deuteron and ionized particles self space charge forces increases and become the same order of magnitude as external one. If we are not taking

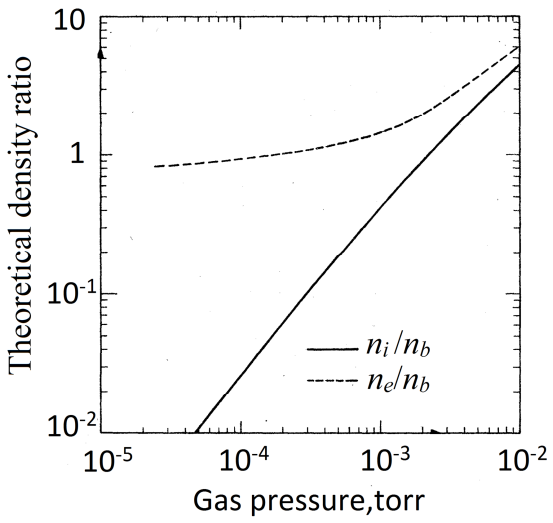

Figure 8: Ratio of electron n_e or ion n_i densities with respect to deuteron beam n_b density as a function of pressure.

into account ionization processes, deuteron beam propagation for current 150 mA shown on Fig. 12*a*. Injected from ion source deuterons cannot overcome own space charge potential wall and form a virtual cathode positive potential value (see Fig. 13). Significant part of them leave the region in radial direction and get off to focusing electrode. Target current become four time

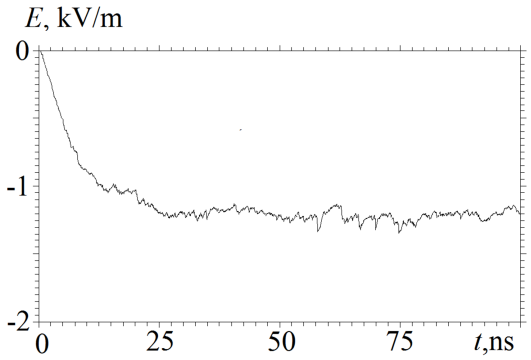

Figure 9: Longitudinal electric self-field time dependence near the cathode.

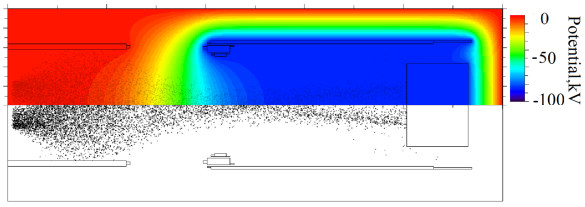

Figure 10: Deuterons distribution (lower) and total field (external and self-field) potential (upper) in neutron tube.

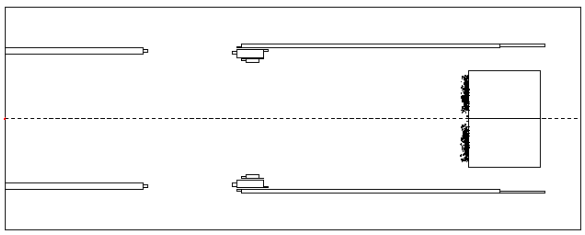

Figure 11: Knocked on electrons distribution.

less than injection one. If we take into account ionization processes deuteron beam propagation changes considerably (see Fig. 12*b*). Electrons, produced by ionization, are trapped within the deuteron beam space charge potential wall and cannot leave the interaction region (see Fig. 14*a*), as they did for current 150 μA (see Fig. 14*b*). Electron accumulation result in decreasing of the potential wall effective depth and deuteron target current rising. Figure 15 shows longitudinal electric field time dependence on the tube axis near the left border for cases without (*a*) and with (*b*) ionization taking into account. The value of deuteron current increases almost three times that result in identical neutron flow Φ increased approximately the same value [Didenko et al., 2012].

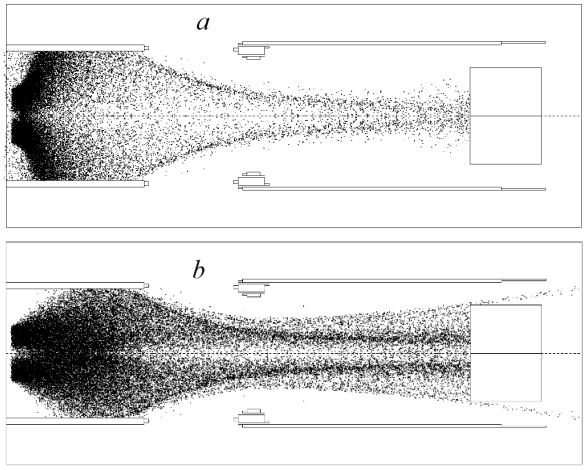

Figure 12: Deuterons distribution without (*a*) and with (*b*) ionization.

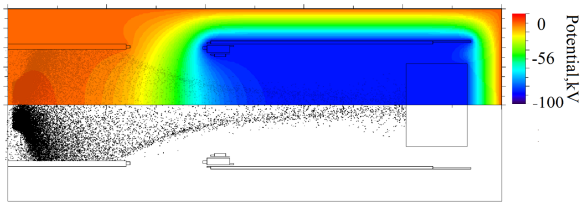

Figure 13: Virtual cathode forming.

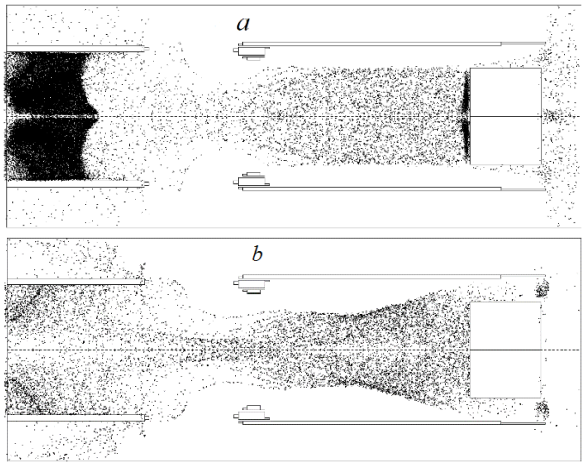

Figure 14: Electrons distributions for current 150 mA (*a*) and 150 μA (*b*).

$$\Phi = \frac{sn}{e\tau} \sum_i q_i \int_0^{W_i} dW \frac{\sigma(W)}{F(W)} \tag{8}$$

where s – target stoichiometry coefficient, n – target nuclei concentration, e – elementary electric charge, q_i - deuteron charge with energy W_i, $\sigma(W)$- nuclei reaction cross-section on the target, $F(W)$ - deuteron

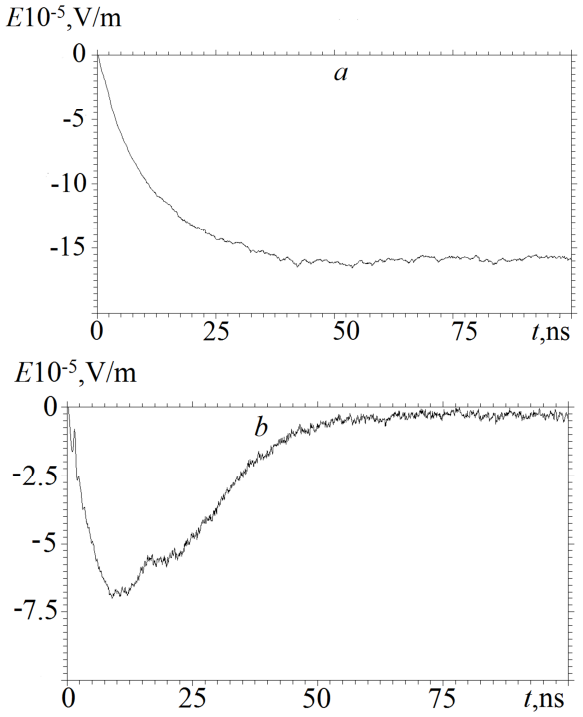

Figure 15: Longitudinal electric field time dependence without (*a*) and with (*b*) ionization taking into account.

bremsstrahlung loss in the target, τ- pulse duration.

Moreover, own longitudinal electric field rise near the target leads to reduction of accelerating electrode — target potential wall and, as a result, additional knocked on electrons may appear in the region. Influence of low energy ion, produced by ionization, is not so significant. Slow ion rather quickly obtain radial velocity and move to the tube periphery (see Fig. 16).

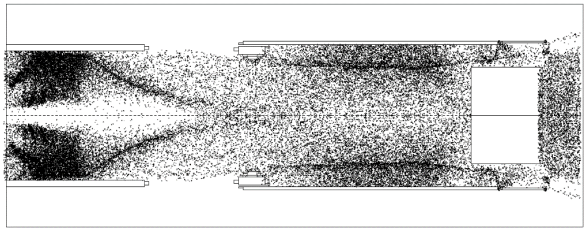

Figure 16: Slow ion distributions in the tube.

5 Conclusion

Thus, space charge neutralization of deuteron beams by electrons, produced by ionization, may considerably increase target current and, as a result, output neutron flow.

References

Belikh, S.F., Evtukhov, R.N., Lutkova, L.V et al. (1992) Luminous ion beams use for ion-optic system characteristic measurement. *Journal of Technical Physics* **62**(6), pp. 179–188.

Didenko, A.N., Rashchikov, V.I., and Fortov, V.E. (2011) Mechanism of Generation of High Intensity Terahetrz Radiation under the Action of High Power Laser Pulsed on a Target. *Technical Physics* **56**(10), pp. 1535–1538.

Didenko, A.N., Rashchikov, V.I., Ryzhkov, V.I. et al. (2012) Computer simulation of nanosecond neutron pulse generation in vacuum accelerator tubes *Atomic Energy* **112**(3), pp. 230–234.

Holmes, A.J.T. (1979) Theoretical and experimental study of space charge in intense ion beams. In *Phys. Rev. A.* **19**(1), pp. 389–407.

Rashchikov, V.I.(1990) Electromagnetic field calculation in complex geometry structures. *Problems of Atomic Science and Technology. Series: Nuclear Physics Investigations* **10**(18), pp. 50–53.